Since January 2020 Elsevier has created a COVID-19 resource centre with free information in English and Mandarin on the novel coronavirus COVID-19. The COVID-19 resource centre is hosted on Elsevier Connect, the company's public news and information website.

Antiviral Research 147 (2017) 58–66

Contents lists available at ScienceDirect

Antiviral Research

journal homepage: www.elsevier.com/locate/antiviral

Inhibition of rubella virus replication by the broad-spectrum drug nitazoxanide in cell culture and in a patient with a primary immune deficiency

Ludmila Perelygina[a], Timo Hautala[b], Mikko Seppänen[c], Adebola Adebayo[a], Kathleen E. Sullivan[d], Joseph Icenogle[a,*]

[a] Division of Viral Diseases, Centers for Disease Control and Prevention, 1600 Clifton Rd NE, MS C22, Atlanta, GA 30333, USA
[b] Department of Internal Medicine, Oulu University Hospital, Kajaanintie 50, 90220 Oulu, Finland
[c] Immunodeficiency Unit, Inflammation Center and Center for Rare Diseases, Children's Hospital, Helsinki University and Helsinki University Hospital, Helsinki, Finland
[d] Division of Allergy and Immunology, The Children's Hospital of Philadelphia, 3615 Civic Center Blvd., Philadelphia, PA 19104, USA

ARTICLE INFO

Keywords:
Rubella virus
Antivirals
Nitazoxanide
Patient with primary immune deficiency
Rubella-positive granuloma

ABSTRACT

Persistent rubella virus (RV) infection has been associated with various pathologies such as congenital rubella syndrome, Fuchs's uveitis, and cutaneous granulomas in patients with primary immune deficiencies (PID). Currently there are no drugs to treat RV infections. Nitazoxanide (NTZ) is an FDA-approved drug for parasitic infections, and has been recently shown to have broad-spectrum antiviral activities. Here we found that empiric 2-month therapy with oral NTZ was associated in the decline/elimination of RV antigen from lesions in a PID patient with RV positive granulomas, while peginterferon treatment had no effect. In addition, we characterized the effects of NTZ on cell culture models of persistent RV infection. NTZ significantly inhibited RV replication in a primary culture of human umbilical vein endothelial cells (HUVEC) and Vero and A549 epithelial cell lines in a dose dependent manner with an average 50% inhibitory concentration of 0.35 μg/ml (1.1 μM). RV strains representing currently circulating genotypes were inhibited to a similar extent. NTZ affected early and late stages of infection by inhibiting synthesis of cellular and RV RNA and interfering with intracellular trafficking of the RV surface glycoproteins, E1 and E2. These results suggest a potential application of NTZ for the treatment of persistent rubella infections, but more studies are required.

1. Introduction

Rubella virus (RV) is a small, enveloped virus with a positive single-stranded RNA genome (family *Togaviridae*, genus *Rubivirus*). RV is an important human pathogen because of its ability to cause multiple pathologies after establishing persistent infections in immune privileged body sites or in fetuses during the first trimester of pregnancy. Persistent infections in a fetus, which has an immature immune system, can result in multiple birth defects called congenital rubella syndrome (CRS) (Driscoll, 1969; Plotkin et al., 2011; Tondury and Smith, 1966). Post-rubella encephalitis, often fatal, has been documented following persistent infections in the brain with both wild type and vaccine viruses (Chaari et al., 2014; Guler et al., 2009; Wolinsky et al., 1982). Chronic recurrent rubella-associated arthritis can develop after immunization of adults (Fraser et al., 1983; Tingle et al., 1985). Granulomas in persons with primary immune deficiencies (PID) and Fuchs's uveitis are newly suggested diseases associated with decades-long persistent RV infections (Abernathy et al., 2015; Bodemer et al., 2014; Doan et al., 2016; Perelygina et al., 2016). Currently, there are no antiviral drugs to treat rubella infections and identification of treatments for chronic rubella diseases will be beneficial.

Nitazoxanide (NTZ) is an FDA-approved drug (licensed in US as Alinia®) for treatment of enteritides due to parasites, protozoa, and anaerobic bacteria (Cohen, 2005; Fox and Saravolatz, 2005). NTZ was also shown to have broad-spectrum antiviral activities and is currently in Phase II/III clinical trials for hepatitis C, influenza viruses, rotavirus and norovirus (Korba et al., 2008; Rossignol, 2014; Rossignol et al., 2009). No significant drug-related health issues have been reported; the drug is safe and is approved for pediatric use (Cohen, 2005; Fox and Saravolatz, 2005). NTZ targets host functions that are essential for viral replication, but are not pathogen-specific. Several anti-viral mechanisms have been proposed such as induction of innate immunity, downregulation of viral receptors or interference with maturation of viral structural proteins at the post-translational stage, probably due to

* Corresponding author.
E-mail address: jci1@cdc.gov (J. Icenogle).

http://dx.doi.org/10.1016/j.antiviral.2017.09.019
Received 5 July 2017; Received in revised form 25 September 2017; Accepted 29 September 2017
Available online 30 September 2017

Ca2+ depletion inducing chronic sub-lethal stress in the endoplasmic reticulum (ER) (Ashiru et al., 2014; Elazar et al., 2009; Gekonge et al., 2015; Korba et al., 2008; La Frazia et al., 2013; Rossignol et al., 2009; Trabattoni et al., 2016).

In this study, we investigated the ability of NTZ to control RV replication in cell culture and explored the mechanisms of the anti-RV activities of NTZ in this system. *In vitro* studies confirmed that NTZ inhibited RV replication and NTZ treatment of a PID patient showed therapeutic efficacy.

2. Material and methods

2.1. Cell cultures, viruses and treatments

Human umbilical vein endothelial cells (HUVEC) (Lonza) were cultured in Endothelial Growth Medium (Lonza). A549 (ATCC #CCL185) and Vero cells (ATCC #CCL CCL81) were maintained in Dulbecco's Modified Eagle Medium (Invitrogen) containing 5% FBS (Atlanta Biologicals) supplemented with 50 μg/ml gentamicin (Invitrogen). The vaccine strain RA27/3 and clinical isolates RVi/Dezhou. CHN/0.02 (RV-Dz), RVi/Seattle. WA.USA/16.00, RVi/Burlington. MA.USA/44.11, RVi/Yavapai. AZ.USA/4.10, and RVi/Redmond. WA.USA/18.11 were propagated in Vero cells. Nitazoxanide (Sigma-Aldrich) was dissolved in dimethyl sulfoxide (DMSO) at a concentration of 10 mg/ml. Medium containing 0.1% DMSO was used as a vehicle control in all experiments.

2.2. Case description

A female patient born in 1986 had received immunization against measles and rubella at ages 5 and 9 years. Later, she was diagnosed as having combined immunodeficiency involving defective B- and T-cell maturation and she had received immunoglobulin replacement treatments. Since 1999, the patient had suffered from chronic skin lesions of her right hand and arm. Bone and skin biopsies showed granulomatous histology but no causative infectious agent was identified (Fig. 1A–B). Frequent empiric treatments for bacteria, mycobacteria and fungi were given without any significant benefit. In 2015, she was one of the individuals (patient #1) with PID whose cutaneous granulomas were discovered to be positive for the vaccine RV strain, RA 27/3 (Perelygina et al., 2016). In 2015, the patient developed progressive multifocal leukoencephalopathy (PML) associated with polyomavirus JC (JCV). The effects of peginterferon alfa-2a and NTZ treatments on controlling JCV and modifying the PML course has been described in a separate publication, which also includes the detailed timeline of the treatments and the description of the patient's immune status (Hautala et al., 2017). In February 2016, the patient developed septic aspiration pneumonia resulting in death.

2.3. Ethics statement

Informed consent was obtained from the patient's caregiver by the attending physician accordingly to standards of practice in Finland. This project was determined by CDC to be Non-Human Research because CDC was restricted from access to personal identifying information.

2.4. Cytotoxicity and growth inhibition assay

Cells were seeded into 96-well plates at a density of 2×10^4 cells per well and treated with serially diluted NTZ for 48 h in quadruplicate. NTZ cytotoxicity and growth inhibition was assessed with a LDH-Based cytotoxicity detection kit (Roche) using the modified protocol (Smith et al., 2011).

2.5. Virus infection and titration

Confluent cell monolayers in 48-well plates were infected with RV at an MOI of 5 pfu/ml unless differently specified. After 1-h virus adsorption, the monolayers were washed three times with PBS and then treated with NTZ or DMSO. The supernatants were collected at 48 h post-infection (hpi) and titered on Vero cells by an immunocolorimetric

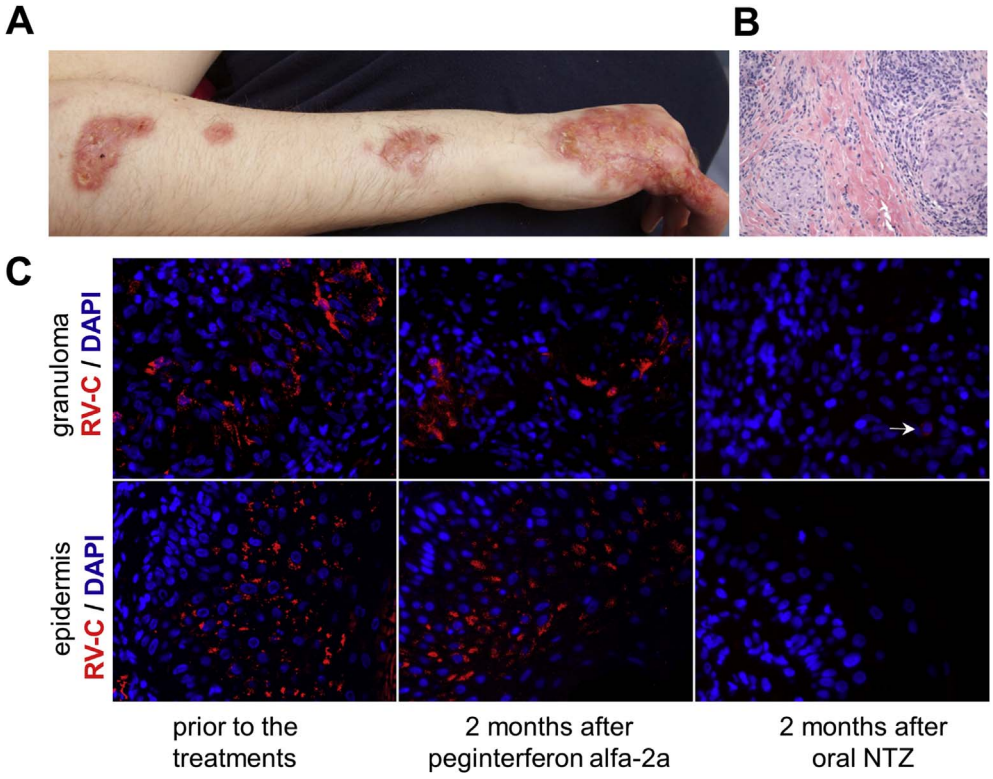

Fig. 1. RV antigen in lesions of a PID patient. (A) Cutaneous skin lesions. (B) Hematoxylin and eosin staining of a cutaneous granuloma. (C) Histological immunofluorescent staining showing distribution of RV capsid protein (red) in granulomas and epidermis of the same skin lesion before and after 2-month treatments with interferon and oral NTZ spaced one month apart. Nuclei were stained with DAPI. Multiple clusters of RV-positive cells were easily detected prior to the NTZ treatment. Note the lack of RV staining in the epidermis and a single weakly positive cell (the white arrow) in the granuloma after the NTZ treatment. (For interpretation of the references to colour in this figure legend, the reader is referred to the web version of this article.)

plaque assay (Chen et al., 2007). NTZ concentrations producing 50% and 90% reductions in virus yield (IC_{50} and IC_{90}) were determined by interpolation from dose-response curves using Prism (v6.0) software (GraphPad Software Inc.). For time-of-addition experiments, HUVEC monolayers were treated with 2.5 μg/ml NTZ for 14, 6 or 3 h before infection, during the 1-h virus adsorption period or at 0, 3, 6, 14, 18, 24 or 48 hpi with RV at an MOI of 5. Virus yield was determined either at 2 dpi (pretreatment of cultures) or 2 days post-treatment.

2.6. RNA fluorescence in situ hybridization (RNA-FISH)

Cells grown on poly-lysine coated chamber slides (BD Biosciences) were infected with RV at an MOI of 5 and then treated with 2.5 μg/ml NTZ for 2 days. RV RNA-FISH using a QuantiGene ViewRNA assay kit (Affymetrix) has been described (Perelygina et al., 2015). A mixture of a Cy5-labeled probe set for either negative or positive-strand RV genomic RNA or influenza negative strand (negative control) and a FITC-labeled probe set for the peptidylpropyl isomerase B (PPIB) or β-actin gene was used. Images were taken using an AxioImager A1 system and AxioVision software (Zeiss, Germany). Fluorescence intensity from six microscopic fields (40–50 cells per field) was measured using ImageJ (Schindelin et al., 2012).

2.7. Labeling nascent RNA

Newly synthesized RNA was detected using a Click-iT RNA imaging kit (Invitrogen) according to manufacturer's instructions. Briefly, cells were treated with either 5 μg/ml NTZ or 0.1% DMSO for 24 h or 10 μg/ml actinomycin D for 4 h followed by 2-h incubation with 2 mM 5-ethynyl uridine. The cells were then fixed with 4% paraformaldehyde, permeabilized with 0.1% triton X-100 and incubated with a Click-iT reaction cocktail containing Alexa Fluor 488-azide. Fluorescence intensity of the nuclei (n = 50 for each condition) in the microscopic images was quantitated using ImageJ.

2.8. Immunofluorescence assay (IFA) and Western blot (WB)

IFA and WB analyses of viral antigens were performed as described (Perelygina et al., 2013) using the mouse monoclonal antibodies specific for rubella capsid protein (Abcam), E2 glycoprotein (Meridian Life Science) and E1 glycoprotein (CDC core facility). The percentage of RV infected cells was quantified by counting E1-positive cells in 10 random microscopic fields.

2.9. Histological immunofluorescence staining of tissue sections

Immunofluorescence staining of formalin fixed paraffin-embedded tissue sections was performed as described earlier (Perelygina et al., 2016).

2.10. Statistical analysis

Statistical analyses were performed with a GraphPad Prizm software (GraphPad Software Inc.) using the Student's *t*-test for unpaired data. A p value of < 0.05 was considered significant.

3. Results

3.1. Decline/elimination of RV from cutaneous lesions of a PID patient

Immunofluorescence staining of the skin biopsies (obtained in 2009, 2011 and 2015) from lesions on the patient's arm revealed the presence of RV antigen in epidermis and cutaneous granulomas (Fig. 1C). In 2015, granulomas progressed and conventional therapies were ineffective. An empiric 2-month antiviral treatment with peginterferon alfa-2a was given according to the hepatitis C regimen (Hoofnagle and Seeff, 2006). The patient was tired, dizzy and lost her appetite when high doses of the drug were given. She also developed thrombocytopenia. The treatment was discontinued due to adverse reactions of the drug. One month later, the patient was given 500 mg of oral NTZ twice daily for two months, which was well tolerated as no obvious negative side-effects were noted. The effectiveness of the treatments was evaluated by immunostaining skin biopsies taken from the same lesion for RV. While the peginterferon treatment had no effect on the amount and distribution of RV antigen, the NTZ treatment resulted in almost complete elimination of RV antigen from the lesions. No antigen was detected in the epidermis and only sporadic, weakly stained macrophages were observed in the sequential sections of the biopsy (Fig. 1C). The treatment did not provide noticeable clinical improvement in the remaining five months of her life. The skin had secondary bacterial infection following the NTZ treatment and the patient was treated with antibiotics.

3.2. Inhibitory effects of NTZ on RV infection

The effect of NTZ treatments on RV replication was investigated using the previously described *in vitro* model of RV persistence, a HUVEC primary culture. HUVEC monolayers were infected with RV-Dz at an MOI of 5 and then treated with different concentrations of NTZ or 0.1% DMSO for 48 h. Virus titers in the medium were determined by a plaque assay. The percentage of infected cells was estimated by counting E1-positive cells following IFA. We observed a dose-dependent inhibition of RV production and a concurrent reduction of the number of RV-positive cells in the NTZ-treated cultures (Fig. 2A–B). There were only a few positive cells in the wells treated with 2.5–5 μg/ml NTZ, while almost all cells were positive in the control wells. No positive cells were observed after the treatment with 10 μg/ml NTZ.

The effects of NTZ treatment on cell viability and proliferation were determined by the LDH assay in uninfected HUVECs. NTZ cytotoxicity was less than 5% if cells were treated with less than 10 μg/ml NTZ. However, in concordance with the published results (Ashiru et al., 2014), NTZ was cytostatic at concentrations higher than 3 μg/ml (Fig. 2C–D). Therefore, we used NTZ at 2.5 μg/ml in most subsequent experiments due to its low cytotoxicity, minimal effects on cell proliferation, and inhibition of RV infection.

Next, we compared NTZ effectiveness in different cell types. HUVEC, A549 and Vero cell monolayers were treated with 2-fold serial dilutions of NTZ following RV-Dz infection at an MOI of 5, and viral yields were determined at 48 hpi. The NTZ treatments resulted in a dose-dependent inhibition of virus production in all cultures with comparable IC_{50} values of 0.37 μg/ml [95% CI: 0.27–0.51], 0.44 μg/ml [95% CI: 0.35–0.54], and 0.25 μg/ml [95% CI: 0.23–0.28] for A549, Vero and HUVEC, respectively (Fig. 3). The average IC_{50} value of NTZ against RV was 0.35 μg/ml (1.1 μM). The IC_{90} values were 4.17 μg/ml [95% CI: 1.10–15.92] for A549, 2 μg/ml [95% CI: 1.07–3.73] for Vero and 0.67 μg/ml [95% CI: 0.49–0.92] for HUVEC.

3.3. Effects of NTZ on replication of different RV strains

To determine whether NTZ inhibits infections with different RV strains, we infected HUVEC monolayers with either the RA27/3 vaccine strain or five wild type RVs representing currently circulating genotypes. The infected cultures were treated with 2.5 μg/ml NTZ for 48 h and then virus titers in the media was determined by a plaque assay (Table 1). These data indicate that replication of different RV strains was inhibited to a similar extent.

3.4. Effects of NTZ on low multiplicity infections

HUVECs were infected with RV-Dz or RA27/3 at an MOI of 0.05. At this MOI only a few cells became infected initially. After virus adsorption, the monolayers were treated with 1.25 or 2.5 μg/ml NTZ for 5

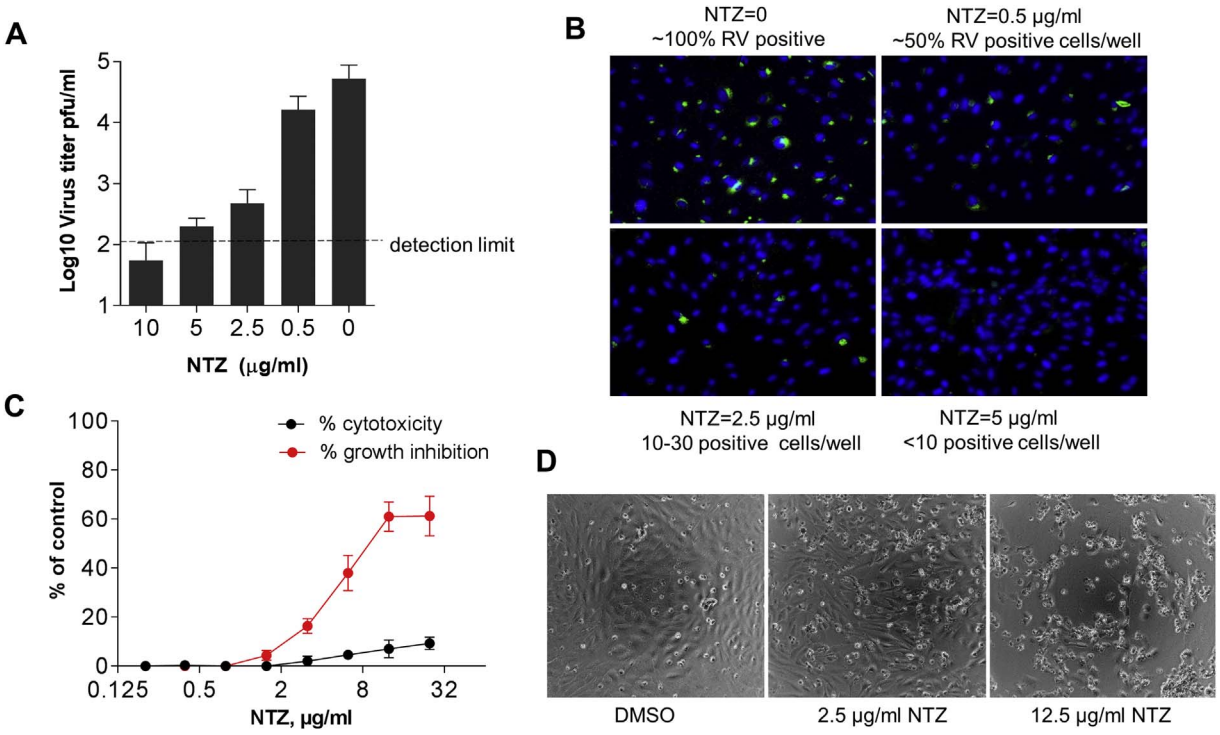

Fig. 2. Antiviral effects of NTZ against RV in HUVECs. Cell monolayers were infected with RV-Dz at an MOI of 5 and then treated with NTZ at the indicated concentrations or vehicle control immediately after adsorption (Panels A and B). (A) Virus titer in the medium was determined at 48 hpi by a plaque assay. The data represent the means ± SD of two independent experiments each done in duplicate. The dashed line shows the lower detection limit of the assay. (B) The monolayers (10^5 cells/well) were fixed at 48 hpi with methanol and immunostained for E1. Nuclei were counterstained with DAPI. HUVECs were treated with different concentrations of NTZ for 48 h (Panels C and D). (C) Cytotoxicity and growth inhibition were analyzed by a modified LDH assay. The data represent the means ± SD of two independent experiments each done in quadruplicate. (D) Phase contrast images of cells showing the effect of different NTZ concentrations on cell viability.

days. Virus titers in the medium were determined by a plaque assay, the percentage of infected cells estimated by IFA. Only a few infected cells were detected in all NTZ-treated wells and the RV yield was substantially inhibited (Table 2). Thus, NTZ prevents RV replication and spread in low multiplicity infections.

3.5. Effects of NTZ on different steps of RV replication

To identify the stage of the RV replication cycle affected by NTZ, time-of-addition experiments were performed using RV infections at an MOI of 5. HUVEC monolayers were treated with 2.5 μg/ml NTZ prior to RV-Dz adsorption, during adsorption only, or post-adsorption. The NTZ treatments prior to adsorption had no effect on RV replication (Fig. 4). Minimal non-significant reduction of the RV yield was observed when the drug was present during the adsorption step suggesting that NTZ does not interfere with virus infectivity and cell entry. The most effective inhibition of RV replication was observed when the treatment was initiated at the early stage of the replication cycle (0–6 hpi). Although less effective, treatments initiated at the later stages (14–24 hpi) were still able to significantly block virus production. These data suggest that NTZ inhibits RV replication at more than one stage of the replication cycle albeit with different efficiencies. However, there was

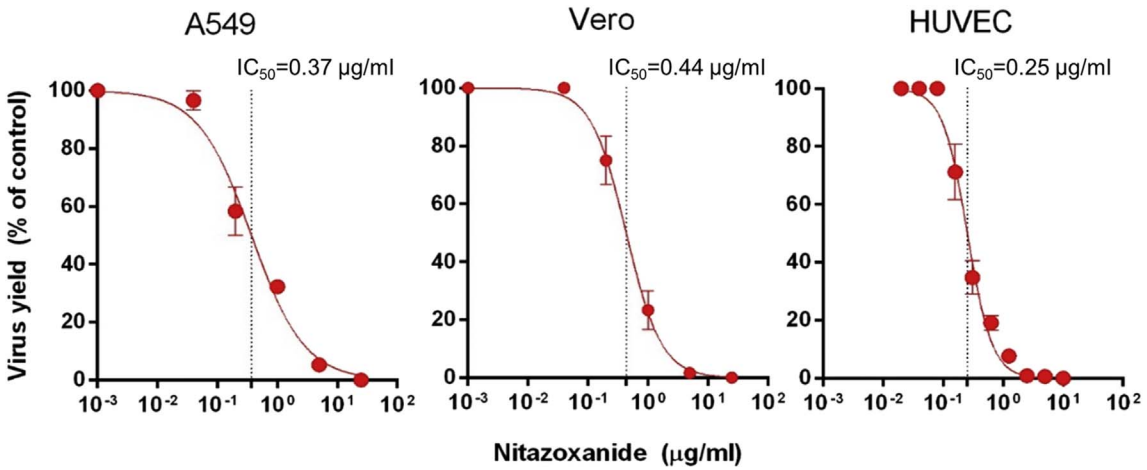

Fig. 3. Dose-dependent effects of NTZ in different cells cultures. A549, Vero or HUVEC monolayers were infected with RV-Dz at an MOI of 5 and then treated with different concentrations of NTZ immediately after virus adsorption. Virus titer in the medium was determined at 48 hpi by a plaque assay. RV-Dz titers in the DMSO-treated cultures (100%) were 7×10^5 (A549), 3×10^5 (Vero), and 6×10^4 (HUVEC). The data, which are expressed as a percentage of untreated control, represent the mean ± SD of two (A549 and Vero) or three (HUVEC) independent experiments each done in duplicate. The dotted lines indicate the IC_{50} values.

Table 1
Sensitivities of vaccine and wild type strains of RV to NTZ (2.5 μg/ml).

RV strain	Genotype	% inhibition[a]
RA27/3[b]	1a	97.0
RVi/Dezhou.CHN/0.02	1E	98.7
RVi/Yavapai.AZ.USA/4.10	1G	99.0
RVi/Seattle.WA.USA/16.00	2B	98.8
RVi/Burlington.MA.USA/44.11	2B	98.5
RVi/Redmond.WA.USA/18.11	2B	98.0

[a] The data are mean of two independent experiments each performed in duplicate.
[b] Vaccine strain.

Table 2
NTZ antiviral effects on infections with low multiplicity (MOI = 0.05 pfu/ml).

RV strain	NTZ	Titer[ab]	Number (%) of infected/total cells[bc]
	μg/ml	pfu/ml	
RV-Dz	2.50	3×10^2	2/320 (0.6%)
	1.25	1×10^3	2/218 (0.8%)
	0.00	3×10^5	252/290 (86.9%)
RA27/3	2.50	$< 10^2$	3/339 (0.8%)
	1.25	3×10^2	3/499 (0.6%)
	0.00	5×10^3	110/440 (23%)

[a] The data are representative of 2 independent experiments, each performed in duplicate.
[b] Virus titer in the media and a number of infected cells were determined at 5 dpi, after multiple rounds of virus replication.
[c] Infected cells were identified by immunostaining for the E1 protein of RV.

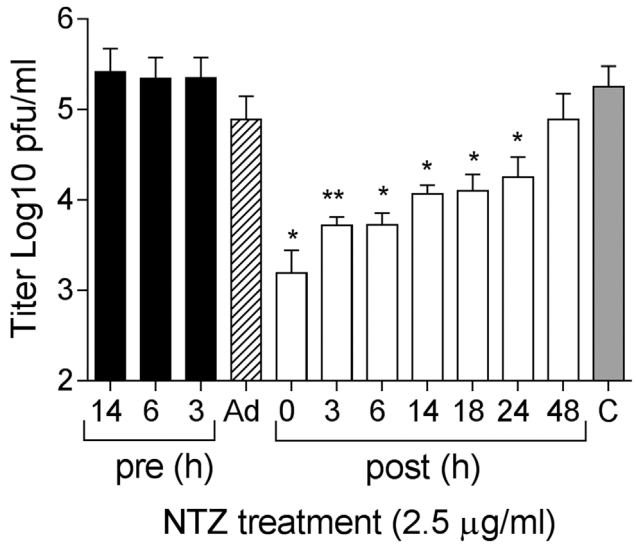

Fig. 4. Effect of NTZ treatment on different stages of RV infection. HUVECs were treated with 2.5 μg/ml NTZ at the indicated times prior (pre, black bars), post infection (post, white bars), or during adsorption only (Ad, the striped bar). The grey bar represents a DMSO control. Virus titers in the medium were determined at 48 hpi (pre, Ad) or 48 h post-treatment. The data represent the means ± SD of at least three independent experiments each done in duplicate. *, $p < 0.05$; **, $p < 0.01$ compared with the DMSO-treated cultures.

no effect if the drug was added at later times (48 hpi).

3.6. Effects of NTZ on synthesis and cellular distribution of RV structural proteins

To assess the effect of NTZ treatment on virus protein synthesis, mock infected or RV-Dz or RA27/3 infected HUVECs were treated with 0.5 and 1 μg/ml NTZ immediately after virus adsorption. At 48 hpi, RV structural proteins were examined by WB analysis. Non-structural proteins were not examined due to the lack of specific antibodies. Large amounts of E1, E2 and C proteins were synthesized in the DMSO-treated RV-Dz or RA27/3 infected cells (Fig. 5A, RV-Dz results are shown). A dose-dependent reduction in viral protein production was observed in the NTZ-treated infected cultures. The lack of changes in the band pattern or band mobility suggested that NTZ does not substantially affect post-translational modifications of the RV structural proteins.

To determine the effect of NTZ on the spatial distribution of RV proteins in infected cells, HUVECs were treated with 1 μg/ml NTZ following infection with RA27/3 at an MOI of 5. At 48 hpi, the RV structural proteins were visualized in the infected cells by immunofluorescence microscopy. There were no differences between the NTZ-treated and control cells in diffuse distribution of C protein in the cytoplasm (not shown). Immunostaining for E1 showed minor changes from tight perinuclear trans-Golgi localization in the control cells to more diffuse perinuclear localization in the NTZ-treated cells (Fig. 5B). The cellular distribution of E2 changed from a co-localization with E1 in the trans-Golgi in the control cells to a diffuse cytoplasmic distribution in many NTZ-treated cells. In some NTZ-treated cells E2 formed vesicular structures evenly distributed in the cytoplasm (Fig. 5B). These data suggest that NTZ affects E1-E2 complex formation and intracellular trafficking.

3.7. Effects of NTZ on RNA replication

To investigate whether NTZ effects RV genomic RNA synthesis, we performed an RNA-FISH analysis of the RV-Dz and RA27/3 infected HUVECs after the treatment with 2.5 μg/ml NTZ using the probe sets specific for positive and negative RNA strands. RV + signal (> 50 dots/cell) was detected in the infected control cells, but it was lacked or substantially reduced in NTZ-treated cells (Fig. 6A–B). In accordance with the reported results (Perelygina et al., 2015), only a 1–3 negative-strand RNA molecules were detected in the control cultures, whereas the RV- hybridization signal in the NTZ-treated cells was less than 1 dot/cell (Fig. 6A, RV-Dz results shown), which was the same as the signal produced by the influenza probe set (not shown). These data suggest that NTZ inhibits synthesis of the both positive and negative strands of RV RNA.

Interestingly, the amounts of GAPDH mRNA (a positive assay control) were also substantially reduced in the NTZ-treated cultures (Fig. 6A). We confirmed these results using a different reference gene, β-actin (Fig. 6B). Quantitation of the fluorescence intensities by ImageJ revealed 5–6 fold reduction of both GAPDH and β-actin RNA signals (Fig. 6C). These results suggested either inhibition of cellular RNA synthesis by NTZ or activation of an RNA degradation pathway such as RNAseL. To further test this hypothesis, cell monolayers were treated with either 5 μg/ml NTZ, 0.1% DMSO or 10 μg/ml actinomycin D (inhibitor of cellular transcription) and then nascent RNA was fluorescently labeled using RNA-click chemistry. Analysis of microscopic images showed that the size and fluorescence intensity in nucleoli (region of ribosomal RNA synthesis) were decreased after the NTZ treatment (Fig. 7A). Total nascent RNA levels per nucleus determined by quantitation of the fluorescence intensity of nuclei (n = 50 for each condition) with ImageJ were found to be reduced by ~30% in the NTZ-treated samples compared to the levels in the control samples (Fig. 7B). Thus, NTZ inhibits synthesis of both viral and cellular RNA.

4. Discussion

We observed the apparent effectiveness of NTZ and the lack of effectiveness of interferon therapy in a single PID patient with severe skin granulomas positive for RV antigen. Two-month peginterferon treatment, which was given prior to NTZ, did not eliminate or reduce the amount of RV antigen in the lesions of this patient. The inability of interferon-alpha therapies to reduce RV excretion has been also reported in infants with congenital rubella syndrome (Arvin et al., 1982).

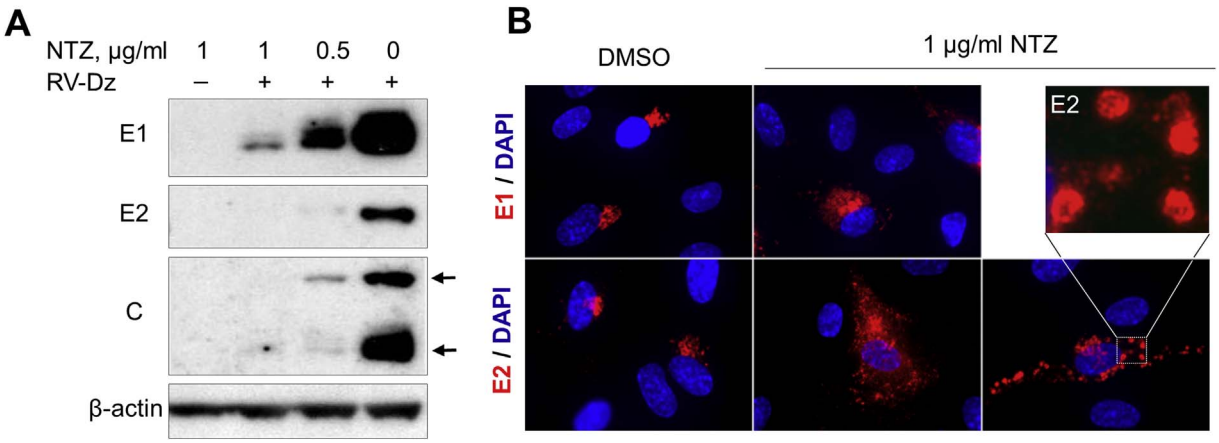

Fig. 5. Effects of NTZ on RV proteins in HUVECs. (A) WB analysis of rubella structural proteins. HUVECs were infected with RV-Dz at an MOI of 5 or mock-infected and then exposed to 0.5 or 1 μg/ml NTZ or vehicle for 48 h. Proteins were extracted with RIPA buffer, separated by a 4–12% non-reducing NuPage gel, and then the blots were probed with rubella specific antibodies to identify RV structural proteins E1, E2 and C (two C bands indicated by the arrows). The blots were also probed with β-actin MAb to demonstrate equal protein loading. (B) Immunofluorescence analysis (at 2 dpi) of rubella structural proteins in the HUVEC monolayers that were treated with 1 μg/ml NTZ following infection with RA27/3 (MOI = 5 pfu/well). Insert represents enlarged image of the E2 globular structures. Representative results of two independent experiments are shown in both A and B.

Following treatment with 500 mg oral NTZ for two months, RV was cleared from the wounds of the patient, but no clinical improvement was observed. There are several possible reasons for that. First of all, although the association between skin granulomas and RV infection has been clearly demonstrated in individuals with some primary immune deficiencies (Bodemer et al., 2014; Perelygina et al., 2016), the causal role of RV infection in the formation of granulomas has not yet been proven. However, the absence of RV RNA in the unaffected skin ((Bodemer et al., 2014); our unpublished observations) and detection of RV in granulomas in the internal organs of some PID patients ((Neven et al., 2017); our unpublished observations) suggest the causality. Of course, with lesions that develop years or even decades after vaccination, causality determinations will likely require prospective studies with long-term follow up. The patient had a very advanced/extensive case. Her lesions had have persisted for more than a decade, and so one would expect it to take a long time to reach complete clinical or histological cure after elimination of the foreign antigen, at best. Furthermore, this chronic infection may have caused long-term or,

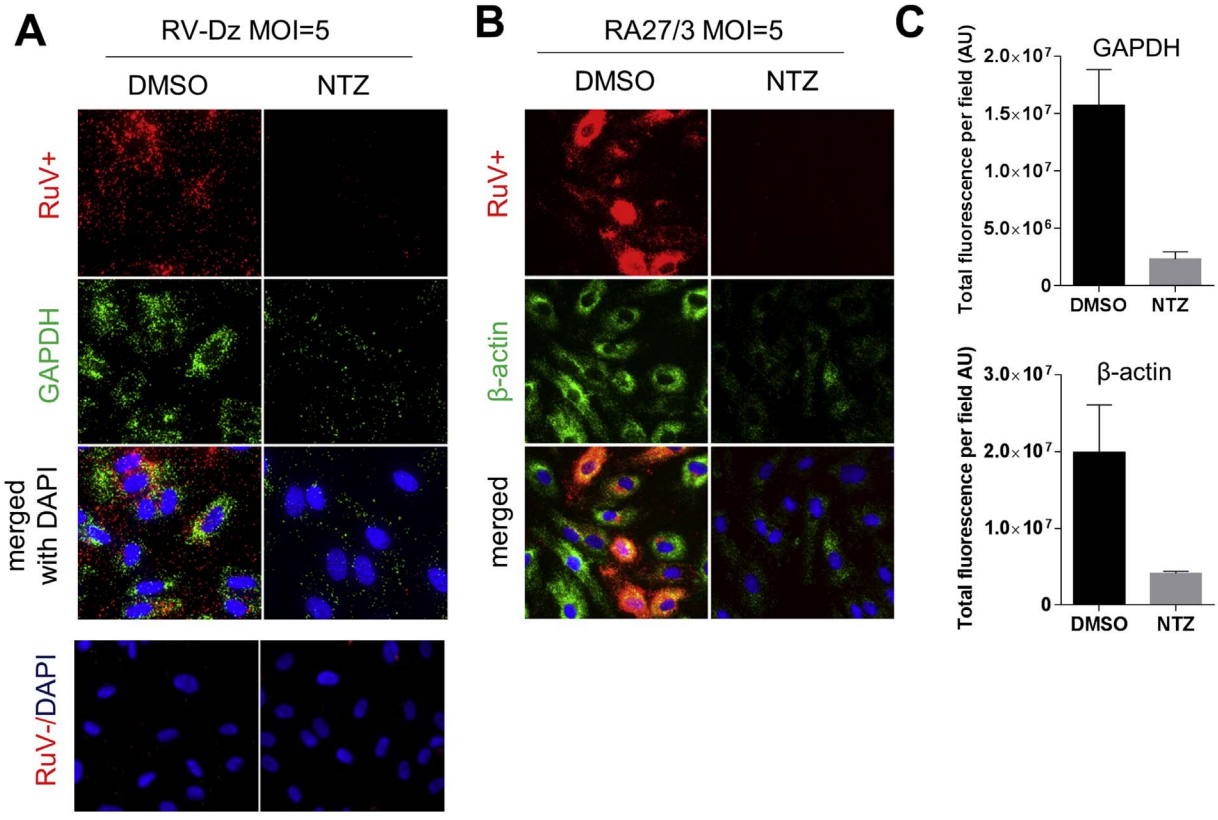

Fig. 6. Inhibition of genomic RV RNA synthesis by NTZ. HUVEC monolayers were infected with RV-Dz (A) or RA27/3 (B) at an MOI of 5 and then exposed to 2.5 μg/ml NTZ or vehicle for 48 h (A and B) Positive or negative strand RV RNA (red) and mRNA for GAPDH and β-actin (green) were detected by RNA-FISH. Nuclei were stained with DAPI. (C) Total fluorescence of each of six randomly picked macroscopic fields per each condition was determined by using ImageJ. Data are presented as a mean ± SD of fluorescence intensity in arbitrary units (AU) per a field. (For interpretation of the references to colour in this figure legend, the reader is referred to the web version of this article.)

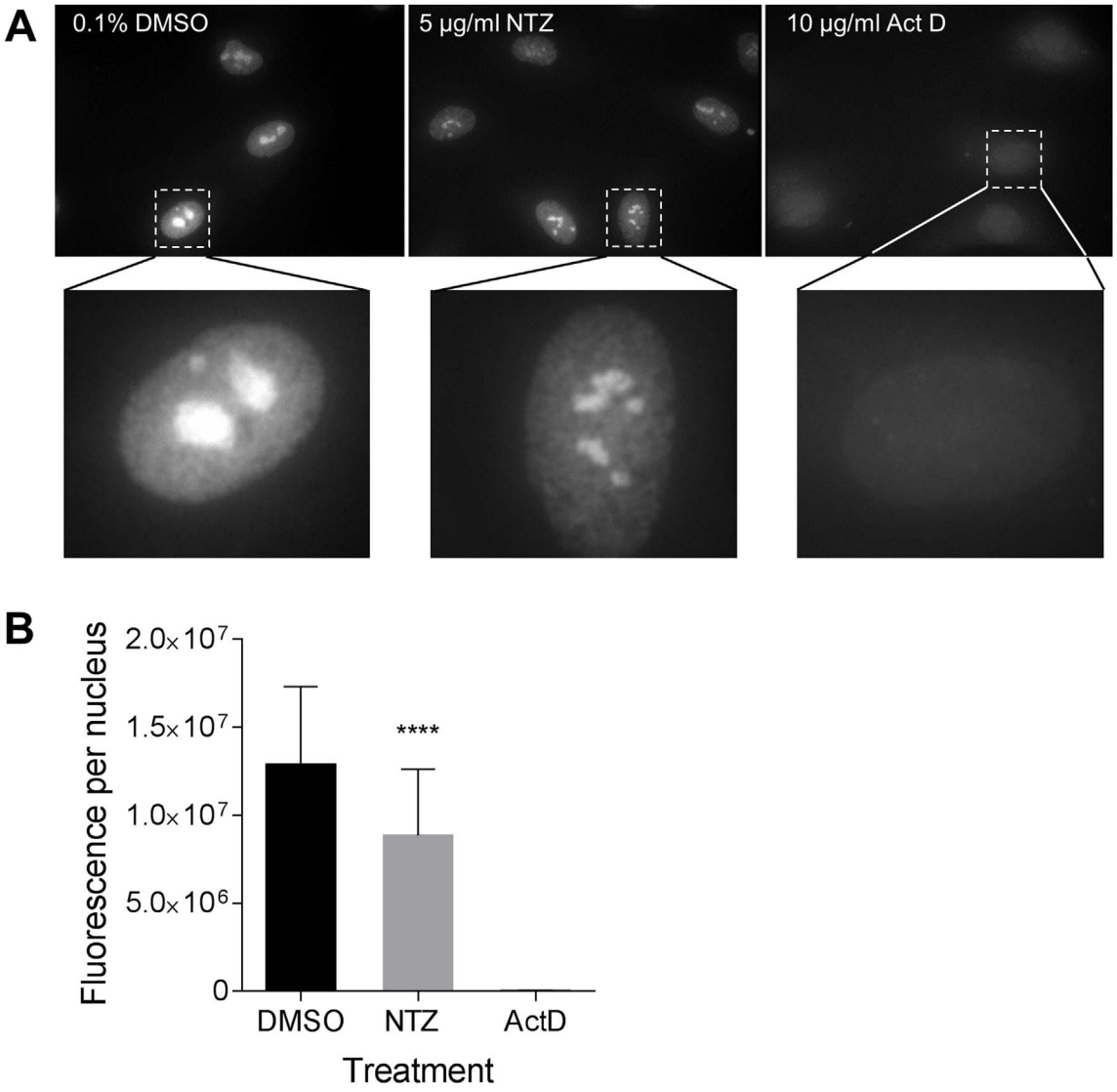

Fig. 7. Inhibition of nascent cellular RNA synthesis by NTZ. (A) HUVEC monolayers were treated with 5 μg/ml of NTZ or DMSO for 24 h. For a positive control, the cells were treated with an inhibitor of cellular RNA transcription, actinomycin D (ActD, 10 μg/ml) for 4 h. Following the treatments, the cells were metabolically labeled with 2 mM 5-ethynyl uridine. Newly synthesized RNA was detected by using click chemistry with azide-derivatized Alexa Fluor 488. Images were acquired using a Zeiss fluorescent microscope. Inserts represent enlarged images of the nuclei. Note the reduced total fluorescence intensity of the nuclei following the NTZ treatment in comparison to a vehicle control and the size reduction and dispersion of nucleoli (ribosomal RNA) in the NTZ treated cells. (B) Total fluorescence of each nucleus was determined using ImageJ. The averages (n = 50 nuclei for each condition) and standard deviation of the mean are shown. ****, $p < 0.0001$.

perhaps, permanent damage to the skin. In addition, secondary bacterial skin infection after the NTZ treatment may also have interfered with the healing process. However, an NTZ treatment may be effective in stopping the development in newly-formed lesions and preventing RV spread and subsequent formation of granulomas in new locations.

We further confirmed NTZ anti-rubella activities *in vitro* and investigated molecular mechanisms of NTZ anti-rubella action using a cell culture model. We documented a dose-dependent inhibitory effect of NTZ on RV infection that is independent of viral strain. The IC_{50} value was determined to be about 0.35 μg/ml (1.1 μM), which is similar to NTZ IC_{50} values for other viruses such as influenza, coronavirus, or hepatitis C (ranging from 0.2 to 1.5 μg/ml), indicating good antiviral activity of the drug (Rossignol, 2014).

We also demonstrated that NTZ suppresses multiple post-entry stages of RV infection as it was observed for other viruses (La Frazia et al., 2013; Shi et al., 2014; Wang et al., 2016). It was more effective at the early stages of the replication cycle and completely blocked RV infection at 10 μg/ml, the peak concentration of the drug (C_{max}) in human plasma after receiving a single 500-mg oral dose of NTZ (Broekhuysen et al., 2000); Alinia® package insert.

Presently, anti-viral mechanisms of NTZ are not fully elucidated. Since NTZ inhibits replication of various DNA viruses and RNA viruses that use different replication strategies, it was suggested that cellular pathways (e.g., cap-mediated translation, ER-to-Golgi trafficking or intracellular Ca^{2+} regulatory pathways) might be affected rather than virus-specific targets (Ashiru et al., 2014; Elazar et al., 2009; Rossignol et al., 2009). Here we show that the level of cellular RNA transcription in NTZ-treated cells was reduced by more than 30% and the level of some cellular mRNAs may drop several-fold.

We have also demonstrated that synthesis of both negative and positive RNA strands of RV was substantially inhibited. Inhibition of viral RNA replication by NTZ was also reported for Japanese encephalitis (JE) virus (Shi et al., 2014). However, for other viruses, e.g. influenza and hepatitis B virus, inhibition of synthesis of viral genomes has not been detected and NTZ has been shown to act at post-translational level by blocking maturation and trafficking of envelope glycoproteins of these viruses (Rossignol et al., 2009; Stachulski et al., 2011). Since viral RNA replication and transcription depend on multiple

cellular accessory proteins of the cellular RNA polymerase (Lai, 1998), NTZ interference with viral and cellular RNA synthesis could be a molecular mechanism that may mediate NTZ anti-viral actions against RV, like JE.

Replication of RV RNA starts with the production of the negative-strand RNA template and then switches to synthesis of positive-strand genomic and subgenomic RNA at about 10 hpi (Liang and Gillam, 2001). RV was estimated to produce ~ 1–4 copies of negative-strand RNA per a cell (Perelygina et al., 2015) and thus negative-strand RNA synthesis may be more sensitive to inhibitors of RNA replication than positive-strand RNA synthesis. That could explain why NTZ was most effective when administered soon after RV infection.

We also demonstrated that NTZ could block RV production at the late stages of infection (14–24 hpi) probably by affecting E1-E2 complex formation and/or ER-to-Golgi trafficking. E1 and E2 must form correctly folded heterodimers in ER in order to be exported to the Golgi where RV particles assemble (Hobman et al., 1993). NTZ was shown to deplete Ca^{2+} in ER, resulting in perturbation of folding and maturation of secreted and transmembrane proteins and their transfer within ER or ER-Golgi export (Ashiru et al., 2014). We demonstrated the lack of a co-localization of the large proportion of E2 with E1 suggesting perturbed E1-E2 complex formation. Altered localization of structural proteins would be anticipated to have negative effect on virion assembly. Despite its negative effects on multiple cellular pathways, a standard oral dose of NTZ was well tolerated by the PID patient with RV positive granuloma during two-month therapy. NTZ was shown to be safe for both children and adults in several placebo-controlled clinical trials; the rates of occurrence of adverse events did not differ significantly between NTZ and placebo treated groups (Amadi et al., 2002; Haffizulla et al., 2014; Rossignol, 2014).

It is currently unclear whether the identified cellular mechanisms were responsible for the reduction of RV antigen in the patient lesions. For example, immunomodulatory effects of NTZ (Hong et al., 2012; Trabattoni et al., 2016) may have played a role. Following oral administration, NTZ is rapidly adsorbed in the gastrointestinal tract and then hydrolyzed to form tizoxanide (desacetyl nitazoxanide), which is further metabolized to form tizoxanide glucuronide (Broekhuysen et al., 2000). Tizoxanide is at least as active *in vitro* as NTZ against different viruses, while tizoxanide glucuronide exhibits only moderate antiviral activities (Korba et al., 2008; La Frazia et al., 2013; Rossignol, 2009). Second-generation thiazolides with favorable pharmacokinetics and improved antiviral activities are currently under development and evaluation (Keeffe and Rossignol, 2009). Future testing of active NTZ metabolites and new generation thiazolides (e.g., RM-5038 and it active derivative RM-4848) should aid in understanding of anti-RV mechanisms of thiazolides *in vivo* and in identification of the most effective anti-RV compounds.

In conclusion, we have demonstrated that NTZ has a potent antiviral activity against RV both in cell culture and in a single patient at the doses used. Our data suggest multiple *in vitro* mechanisms of drug action including inhibition of cellular and viral RNA synthesis and aberrant trafficking of viral structural proteins. NTZ could be the first drug effective for the treatment of persistent rubella infections. The results of this study suggest that further studies are warranted to evaluate the ability of NTZ to control chronic rubella infections.

Disclaimer

The findings and conclusions in this report are those of the authors and do not necessarily represent the official position of the United States Centers for Disease Control and Prevention.

Funding

This work was supported by core funding from the Centers for Disease Control and Prevention, Oulu University Hospital VTR funding (K74809), Finnish Medical Foundation, and Helsinki University Hospital Research Funds (TYH2016131).

References

Abernathy, E., Peairs, R.R., Chen, M.H., Icenogle, J., Namdari, H., 2015. Genomic characterization of a persistent rubella virus from a case of Fuch' uveitis syndrome in a 73 year old man. J. Clin. Virol. 69, 104–109.
Amadi, B., Mwiya, M., Musuku, J., Watuka, A., Sianongo, S., Ayoub, A., Kelly, P., 2002. Effect of nitazoxanide on morbidity and mortality in Zambian children with cryptosporidiosis: a randomised controlled trial. Lancet 360, 1375–1380.
Arvin, A.M., Schmidt, N.J., Cantell, K., Merigan, T.C., 1982. Alpha interferon administration to infants with congenital rubella. Antimicrob. Agents Chemother. 21, 259–261.
Ashiru, O., Howe, J.D., Butters, T.D., 2014. Nitazoxanide, an antiviral thiazolide, depletes ATP-sensitive intracellular Ca(2+) stores. Virology 462–463, 135–148.
Bodemer, C., Sauvage, V., Mahlaoui, N., Cheval, J., Couderc, T., Leclerc-Mercier, S., Debre, M., Pellier, I., Gagnieur, L., Fraitag, S., Fischer, A., Blanche, S., Lecuit, M., Eloit, M., 2014. Live rubella virus vaccine long-term persistence as an antigenic trigger of cutaneous granulomas in patients with primary immunodeficiency. Clin. Microbiol. Infect. 20, O656–O663.
Broekhuysen, J., Stockis, A., Lins, R.L., De Graeve, J., Rossignol, J.F., 2000. Nitazoxanide: pharmacokinetics and metabolism in man. Int. J. Clin. Pharmacol. Ther. 38, 387–394.
Chaari, A., Bahloul, M., Berrajah, L., Ben Kahla, S., Gharbi, N., Karray, H., Bouaziz, M., 2014. Childhood rubella encephalitis: diagnosis, management, and outcome. J. Child. Neurol. 29, 49–53.
Chen, M.H., Zhu, Z., Zhang, Y., Favors, S., Xu, W.B., Featherstone, D.A., Icenogle, J.P., 2007. An indirect immunocolorimetric assay to detect rubella virus infected cells. J. Virol. Methods 146, 414–418.
Cohen, S.A., 2005. Use of nitazoxanide as a new therapeutic option for persistent diarrhea: a pediatric perspective. Curr. Med. Res. Opin. 21, 999–1004.
Doan, T., Wilson, M.R., Crawford, E.D., Chow, E.D., Khan, L.M., Knopp, K.A., O'Donovan, B.D., Xia, D., Hacker, J.K., Stewart, J.M., Gonzales, J.A., Acharya, N.R., DeRisi, J.L., 2016. Illuminating uveitis: metagenomic deep sequencing identifies common and rare pathogens. Genome Med. 8, 90.
Driscoll, S.G., 1969. Histopathology of gestational rubella. Am. J. Dis. Child. 118, 49–53.
Elazar, M., Liu, M., McKenna, S.A., Liu, P., Gehrig, E.A., Puglisi, J.D., Rossignol, J.F., Glenn, J.S., 2009. The anti-hepatitis C agent nitazoxanide induces phosphorylation of eukaryotic initiation factor 2alpha via protein kinase activated by double-stranded RNA activation. Gastroenterology 137, 1827–1835.
Fox, L.M., Saravolatz, L.D., 2005. Nitazoxanide: a new thiazolide antiparasitic agent. Clin. Infect. Dis. 40, 1173–1180.
Fraser, J.R., Cunningham, A.L., Hayes, K., Leach, R., Lunt, R., 1983. Rubella arthritis in adults. Isolation of virus, cytology and other aspects of the synovial reaction. Clin. Exp. Rheumatol. 1, 287–293.
Gekonge, B., Bardin, M.C., Montaner, L.J., 2015. Nitazoxanide inhibits HIV viral replication in monocyte-derived macrophages. AIDS Res. Hum. Retrovir. 31, 237–241.
Guler, E., Davutoglu, M., Guler, S., Citirik, D., Karabiber, H., 2009. Encephalitis in a child during atypical course of rubella. Infection 37, 65–66.
Haffizulla, J., Hartman, A., Hoppers, M., Resnick, H., Samudrala, S., Ginocchio, C., Bardin, M., Rossignol, J.F., Group, U.S.N.I.C.S., 2014. Effect of nitazoxanide in adults and adolescents with acute uncomplicated influenza: a double-blind, randomised, placebo-controlled, phase 2b/3 trial. Lancet Infect. Dis. 14, 609–618.
Hautala, T., Perelygina, L., Vuorinen, V., Hautala, N., Hägg, P., Bode, M., Rusanen, H., Renko, H., Glumoff, V., Schwab, N., Schneider-Hohendorf, T., Murk, J.L., Sullivan, K.E., Seppänen, M., 2017. Nitazoxanide may modify the course of progressive multifocal leukoencephalopathy. J. Clin. Immunol (under final submitted for publication).
Hobman, T.C., Woodward, L., Farquhar, M.G., 1993. The rubella virus E2 and E1 spike glycoproteins are targeted to the Golgi complex. J. Cell Biol. 121, 269–281.
Hong, S.K., Kim, H.J., Song, C.S., Choi, I.S., Lee, J.B., Park, S.Y., 2012. Nitazoxanide suppresses IL-6 production in LPS-stimulated mouse macrophages and TG-injected mice. Int. Immunopharmacol. 13, 23–27.
Hoofnagle, J.H., Seeff, L.B., 2006. Peginterferon and ribavirin for chronic hepatitis C. N. Engl. J. Med. 355, 2444–2451.
Keeffe, E.B., Rossignol, J.F., 2009. Treatment of chronic viral hepatitis with nitazoxanide and second generation thiazolides. World J. Gastroenterol. 15, 1805–1808.
Korba, B.E., Montero, A.B., Farrar, K., Gaye, K., Mukerjee, S., Ayers, M.S., Rossignol, J.F., 2008. Nitazoxanide, tizoxanide and other thiazolides are potent inhibitors of hepatitis B virus and hepatitis C virus replication. Antivir. Res. 77, 56–63.
La Frazia, S., Ciucci, A., Arnoldi, F., Coira, M., Gianferretti, P., Angelini, M., Belardo, G., Burrone, O.R., Rossignol, J.F., Santoro, M.G., 2013. Thiazolides, a new class of antiviral agents effective against rotavirus infection, target viral morphogenesis, inhibiting viroplasm formation. J. Virol. 87, 11096–11106.
Lai, M.M., 1998. Cellular factors in the transcription and replication of viral RNA genomes: a parallel to DNA-dependent RNA transcription. Virology 244, 1–12.
Liang, Y., Gillam, S., 2001. Rubella virus RNA replication is cis-preferential and synthesis of negative- and positive-strand RNAs is regulated by the processing of nonstructural protein. Virology 282, 307–319.
Neven, B., Perot, P., Bruneau, J., Pasquet, M., Ramirez, M., Diana, J.S., Luzi, S., Corre-Catelin, N., Chardot, C., Moshous, D., Leclerc Mercier, S., Mahlaoui, N., Aladjidi, N., Le Bail, B., Lecuit, M., Bodemer, C., Molina, T.J., Blanche, S., Eloit, M., 2017. Cutaneous and visceral chronic granulomatous disease triggered by a rubella virus vaccine strain in children with primary immunodeficiencies. Clin. Infect. Dis. 64,

83–86.
Perelygina, L., Adebayo, A., Metcalfe, M., Icenogle, J., 2015. Differences in establishment of persistence of vaccine and wild type rubella viruses in fetal endothelial cells. PLoS One 10, e0133267.
Perelygina, L., Plotkin, S., Russo, P., Hautala, T., Bonilla, F., Ochs, H.D., Joshi, A., Routes, J., Patel, K., Wehr, C., Icenogle, J., Sullivan, K.E., 2016. Rubella persistence in epidermal keratinocytes and granuloma M2 macrophages in patients with primary immunodeficiencies. J. Allergy Clin. Immunol. 138, 1436–1439 e1411.
Perelygina, L., Zheng, Q., Metcalfe, M., Icenogle, J., 2013. Persistent infection of human fetal endothelial cells with rubella virus. PLoS One 8, e73014.
Plotkin, S., Reef, S., Cooper, L., Alford, C.A., 2011. Rubella. In: R, J., Klein, J., Wilson, C., Nizet, V., Maldonato, Y. (Eds.), Infectious Diseases of the Fetus and Newborn Infant. Elsveier, Philadelphia, PA, pp. 861–898.
Rossignol, J.F., 2009. Thiazolides: a new class of antiviral drugs. Expert Opin. Drug Metab. Toxicol. 5, 667–674.
Rossignol, J.F., 2014. Nitazoxanide: a first-in-class broad-spectrum antiviral agent. Antivir. Res. 110, 94–103.
Rossignol, J.F., La Frazia, S., Chiappa, L., Ciucci, A., Santoro, M.G., 2009. Thiazolides, a new class of anti-influenza molecules targeting viral hemagglutinin at the post-translational level. J. Biol. Chem. 284, 29798–29808.
Schindelin, J., Arganda-Carreras, I., Frise, E., Kaynig, V., Longair, M., Pietzsch, T., Preibisch, S., Rueden, C., Saalfeld, S., Schmid, B., Tinevez, J.Y., White, D.J., Hartenstein, V., Eliceiri, K., Tomancak, P., Cardona, A., 2012. Fiji: an open-source platform for biological-image analysis. Nat. Methods 9, 676–682.
Shi, Z., Wei, J., Deng, X., Li, S., Qiu, Y., Shao, D., Li, B., Zhang, K., Xue, F., Wang, X., Ma, Z., 2014. Nitazoxanide inhibits the replication of Japanese encephalitis virus in cultured cells and in a mouse model. Virol. J. 11, 10.
Smith, S.M., Wunder, M.B., Norris, D.A., Shellman, Y.G., 2011. A simple protocol for using a ldh-based cytotoxicity assay to assess the effects of death and growth inhibition at the same time. PLoS One 6, e26908.
Stachulski, A.V., Pidathala, C., Row, E.C., Sharma, R., Berry, N.G., Lawrenson, A.S., Moores, S.L., Iqbal, M., Bentley, J., Allman, S.A., Edwards, G., Helm, A., Hellier, J., Korba, B.E., Semple, J.E., Rossignol, J.F., 2011. Thiazolides as novel antiviral agents. 2. Inhibition of hepatitis C virus replication. J. Med. Chem. 54, 8670–8680.
Tingle, A.J., Chantler, J.K., Pot, K.H., Paty, D.W., Ford, D.K., 1985. Postpartum rubella immunization: association with development of prolonged arthritis, neurological sequelae, and chronic rubella viremia. J. Infect. Dis. 152, 606–612.
Tondury, G., Smith, D.W., 1966. Fetal rubella pathology. J. Pediatr. 68, 867–879.
Trabattoni, D., Gnudi, F., Ibba, S.V., Saulle, I., Agostini, S., Masetti, M., Biasin, M., Rossignol, J.F., Clerici, M., 2016. Thiazolides elicit anti-viral innate immunity and reduce hiv. Replication. Sci. Rep. 6, 27148.
Wang, Y.M., Lu, J.W., Lin, C.C., Chin, Y.F., Wu, T.Y., Lin, L.I., Lai, Z.Z., Kuo, S.C., Ho, Y.J., 2016. Antiviral activities of niclosamide and nitazoxanide against chikungunya virus entry and transmission. Antivir. Res. 135, 81–90.
Wolinsky, J.S., Waxham, M.N., Hess, J.L., Townsend, J.J., Baringer, J.R., 1982. Immunochemical features of a case of progressive rubella panencephalitis. Clin. Exp. Immunol. 48, 359–366.